Point-Defect-Induced Metastable Phase Diagrams

Maylise Nastar

Université Paris-Saclay, CEA Saclay, SRMP,

F-91191, Gif-sur-Yvette Cedex, France

In coll. with

Liangzhao Huang, Luca Messina, Thomas Schuler,
Kangming Li, ChuChun Fu, Lisa Belkacemi, Quentin Tence
Estelle Meslin, Marie Loyer Prost

Radiation damage starts from a Primary Knock-on Atom

Courtesy of Adrien Couet and Calvin Parkin, Wisconsin University

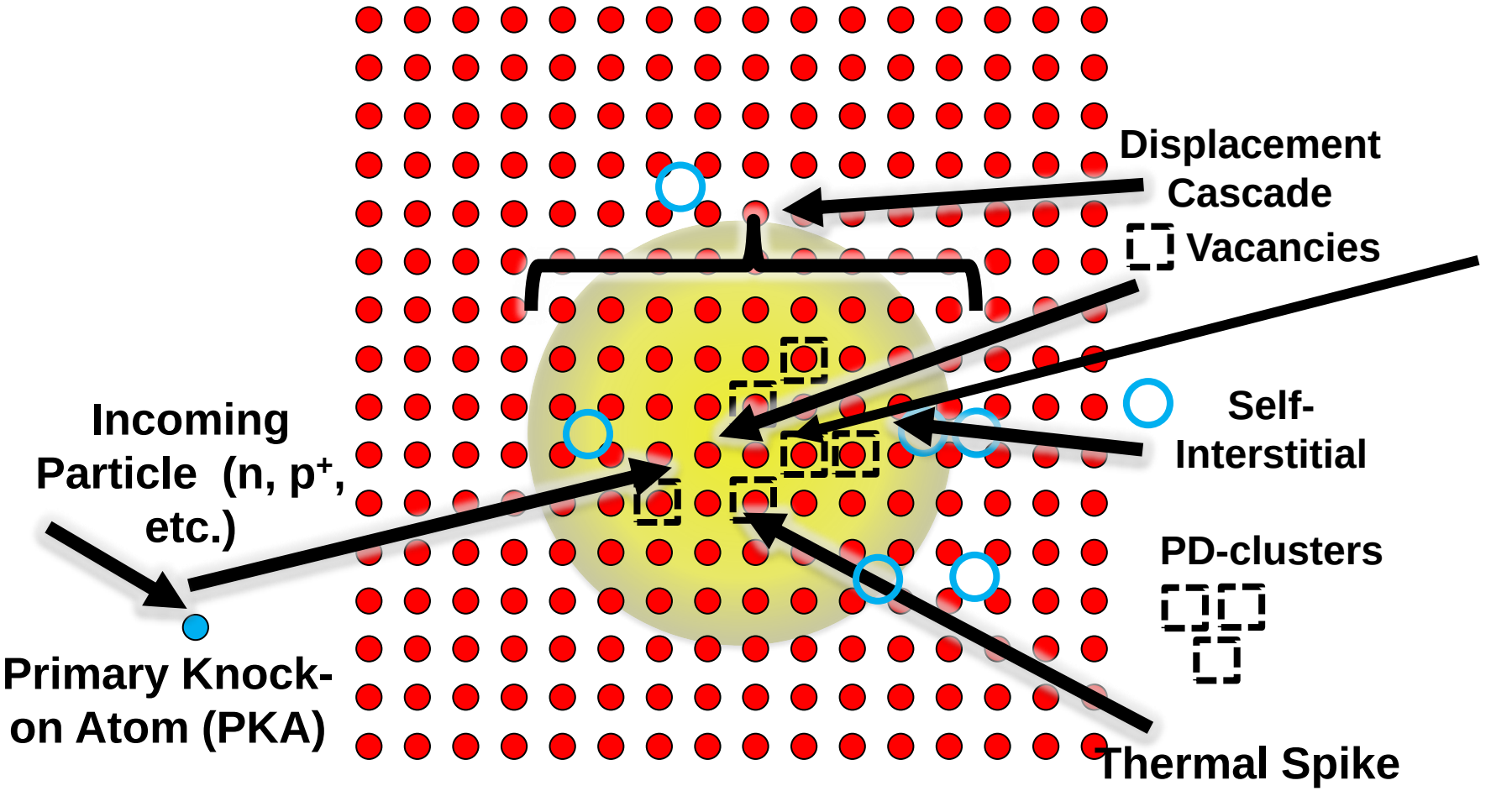

Forced atomic relocation (ballistic mixing in alloys)

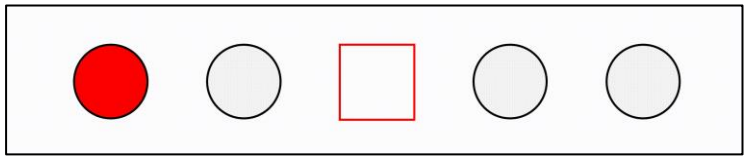

Simulation methods of displacement cascades:
Binary Collision Approximation (SRIM, IRADINA) & Molecular Dynamics methods: damage rate in dpa

Long-term Radiation damage starts from point defect – atom exchanges

Vacancy-atom exchange

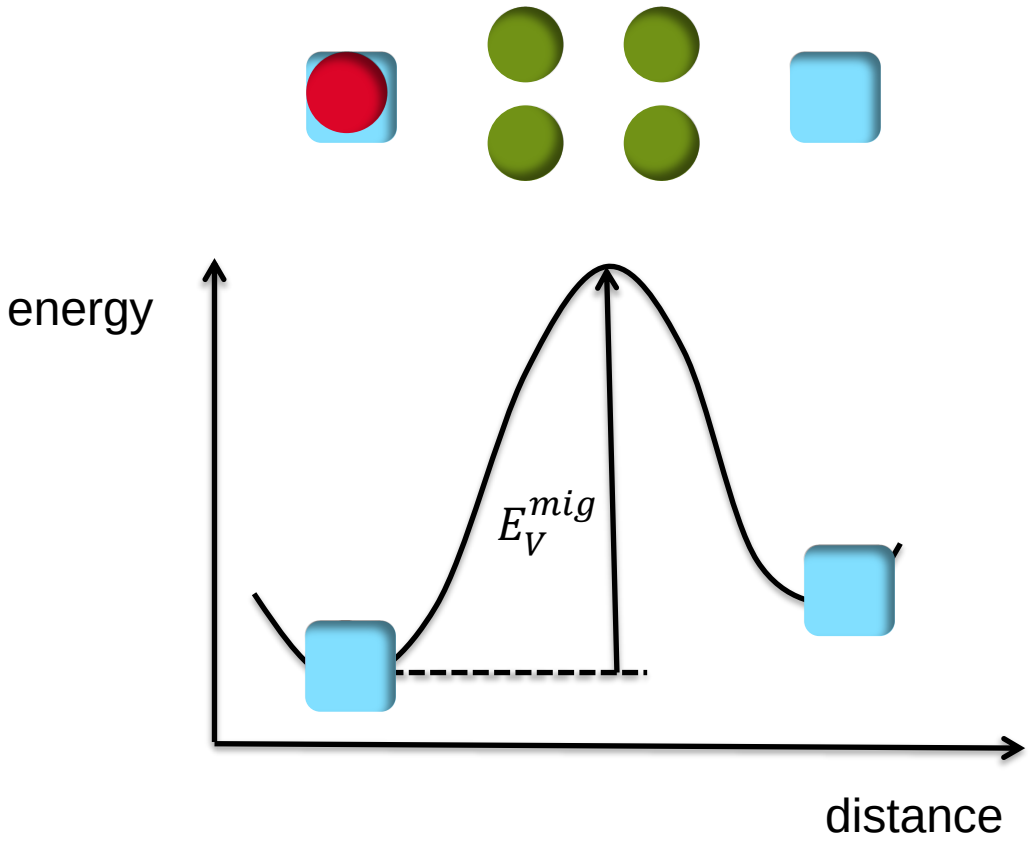

Self-Interstitial-atom exchange: rotation-transl. mechanism

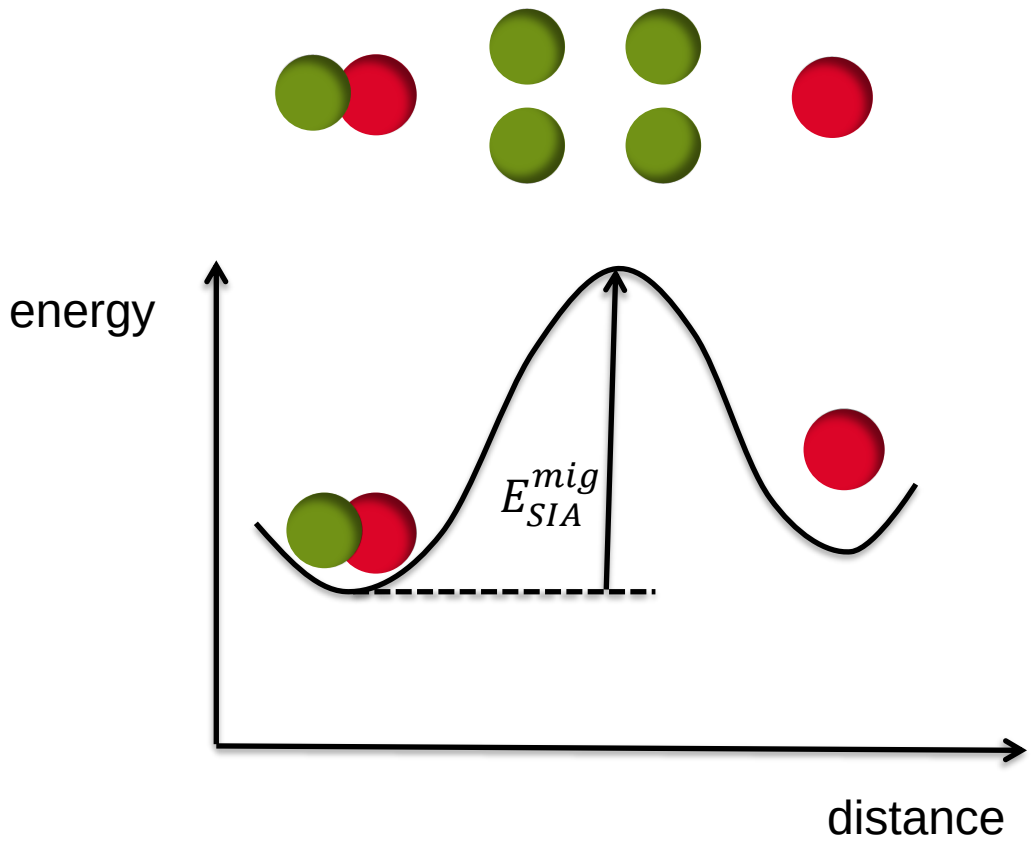

Transition State theory: thermally activated defect-atom exchange≡ $w_{AV} = \nu_A e^{-\frac{E^{mig}}{kT}}$

Microscopic detailed balance of the exchanges tends to local equilibrium

Modeling of long-term radiation damage: can we rely on thermodynamics?

thermally activated diffusion versus a-thermal ballistic mixing, within-cascade defect prod., V-SIA recombination

Constrained thermodynamic based on local equilibrium asumptions

a-thermal event rates << thermal diffusion rates mediated by non-equilibrium defects

- Cluster Onsager diffusion coefficient, Reaction between clusters, precipitation driving forces

- Metastable phase diagrams, Radiation-enhanced diffusion & precipitation, PD clustering

Far from equilibrium diffusion and precipitation a-thermal event rates ≈ thermal diffusion rates
Occurs at low temperature and high radiation flux or in Molecular dynamics FPA or CRA!

- Flux couplings resulting from non-symmetric Onsager matrix & RIS
*Huang, Schuler, Nastar, PRB 100 (2019) 224103
- Ballistic-induced dissolution of secondary-phase precipitates

Outline

- ✓Non-equilibrium defects: diffusion and precipitation driving forces
- ✓Defect-induced dissolution of oxide
- ✓Defect-induced semi-incoherent precipitation
- ✓Defect formation Gibbs free energy from atomic random sampling

Non-equilibrium vacancy concentration under irradiation

*Huang et al., Phys. Rev B 5 (2021), 033605

Mean field Rate theory at steady state

$$\frac{d\bar{C}_V}{dt} = \Phi - K_R(D_V + D_I)\bar{C}_I\bar{C}_V - k^2 D_V(\bar{C}_V - C_V^{eq}) = 0$$

$$\frac{d\bar{C}_I}{dt} = \Phi - K_R(D_V + D_I)\bar{C}_I\bar{C}_V - k^2 D_I(\bar{C}_I - C_I^{eq}) = 0$$

Frenkel pair creation [dpa/s]

V-I Recombination

Diffusion & Elimination At sinks (sink strength: k^2)

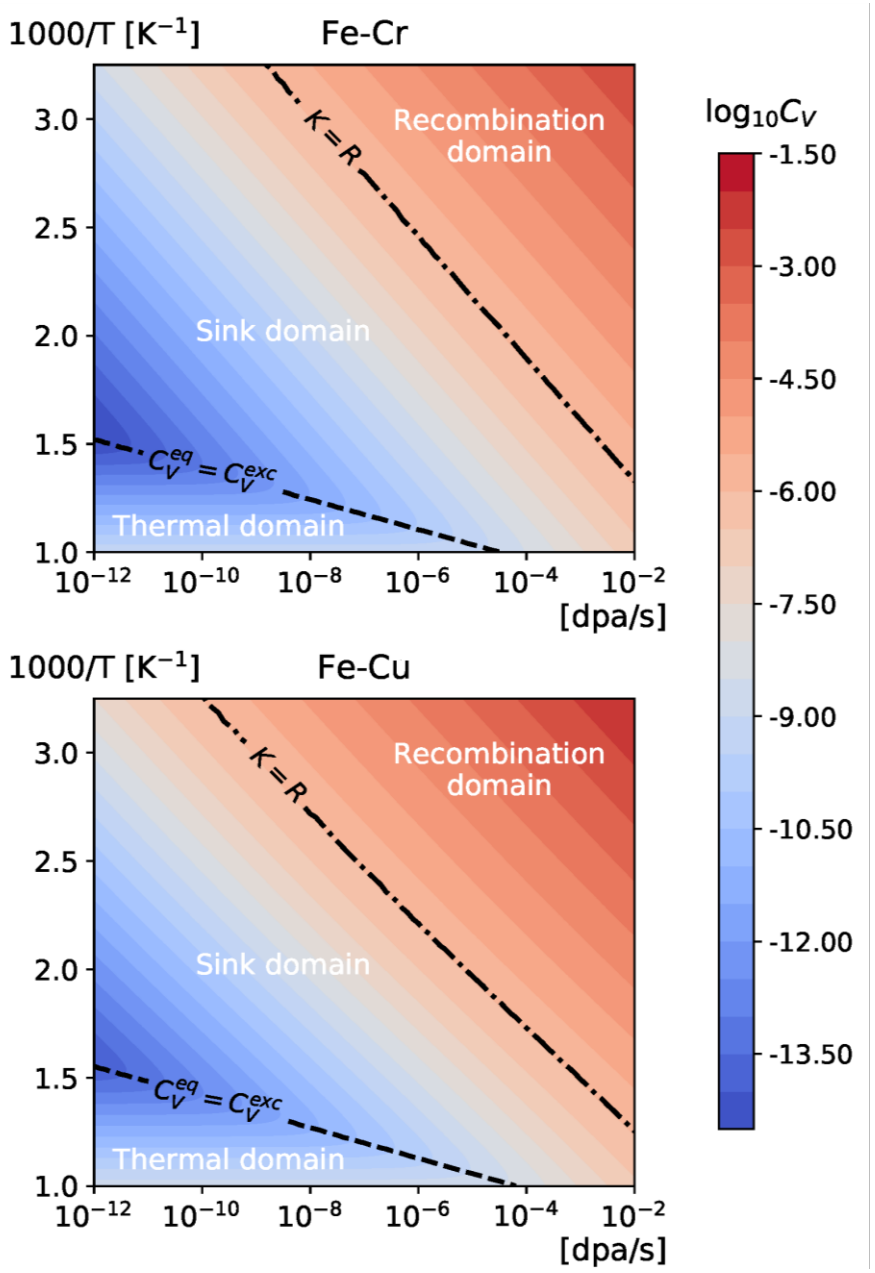

Sink strength: $k^2 = 5.10^{14} m^{-2}$
Solute fraction of Cr or Cu : 1 at. %

Radiation-enhanced diffusion under irradiation

Mean field Rate theory at steady state

$$\frac{d\bar{C}_V}{dt} = \Phi - K_R(D_V + D_I)\bar{C}_I\bar{C}_V - k^2 D_V(\bar{C}_V - C_V^{eq}) = 0$$

$$\frac{d\bar{C}_I}{dt} = \Phi - K_R(D_V + D_I)\bar{C}_I\bar{C}_V - k^2 D_I(\bar{C}_I - C_I^{eq}) = 0$$

Frenkel pair creation [dpa/s]

Diffusion & Elimination At sinks (sink strength: k^2)

Tracer diffusion under irradiation

Mediated by mono-vacancy and mono-SIA

$$D^*_{irr} \approx \bar{C}_V(D^*_{V,thermal}/C_V^{eq}) + \bar{C}_I(D^*_{I,}/C_I^{eq})$$

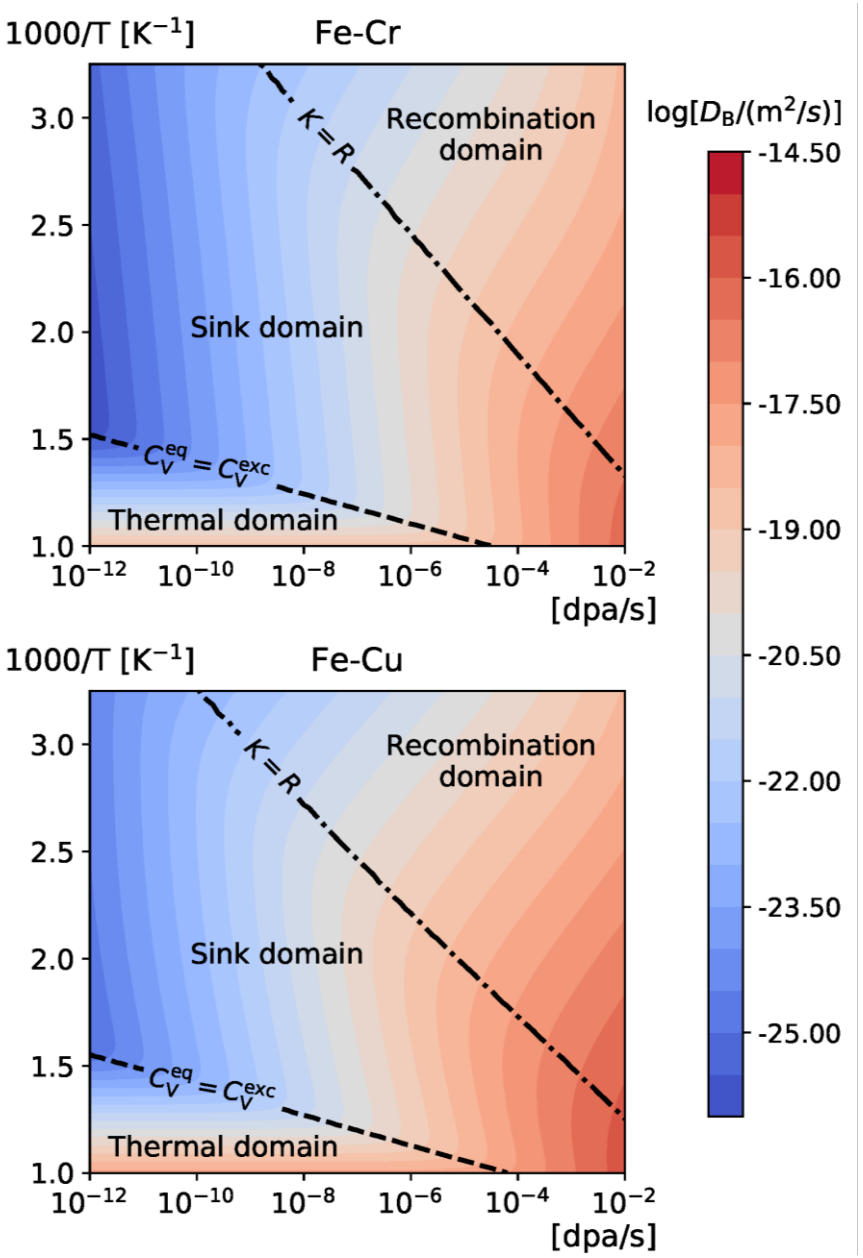

Sink strength: $k^2 = 5.10^{14} m^{-2}$

Solute fraction of Cr or Cu : 1 at. %

Non-eq. point defects acting as non-conservative « chemical » species

Radiation-excitation energy stored in chemical potential of lattice point defect (d)

$$\mu_d = (\partial G/\partial N_d)_{(P,T,N)} = G_{f,d} + k_B T Log(C_d)$$

At equilibirum: $\mu_d = 0$ and $C_d^{eq} = \exp\left(-G_{f,d}/k_B T\right)$

Non equilibrium state: $\mu_d = k_B T Log\left(C_d/C_d^{eq}\right)$ with C_d (radiation flux, recombination, sink strength k^2, D_d)

C_d^{eq}(temperature, local strain/stress and composition)

Diffusion driving force of defect d under a strain field in binary alloy AB (efficiency of PD sink absoption)

$$\nabla(\mu_d - \mu_A) = \frac{\nabla C_d}{C_d} - \frac{\partial C_d^{\mathrm{eq}}}{\partial C_B}\frac{\nabla C_B}{C_d^{\mathrm{eq}}} - \left(P_{ij}^d/k_B T\right)\nabla\varepsilon_{ij}$$ *L. Huang et al. JNM 570, (2022) 153959*

Point defect as a chemical species interacting with solute atoms (conservative species)

Point defects as a buffer of lattice sites (non conservative species) and chemical species

Vacancy removal: $\Delta G = -\mu_V$ and $\Delta N_{lattice\ sites} = -1$

SIA removal: $\Delta G = -\mu_I$ and $\Delta N_{lattice\ sites} = +1$

Outline

✓Non-equilibrium defects: diffusion and precipitation driving forces

✓Defect-induced dissolution of oxide

✓Defect-induced semi-incoherent precipitation

✓Defect formation Gibbs free energy from atomic random sampling

Stability of oxide particles under electron irrad. In 9Cr-ODS Steels

in situ THT observation of Oxide dissolution,

*F. Li et al./JNM 455 (2014) 724

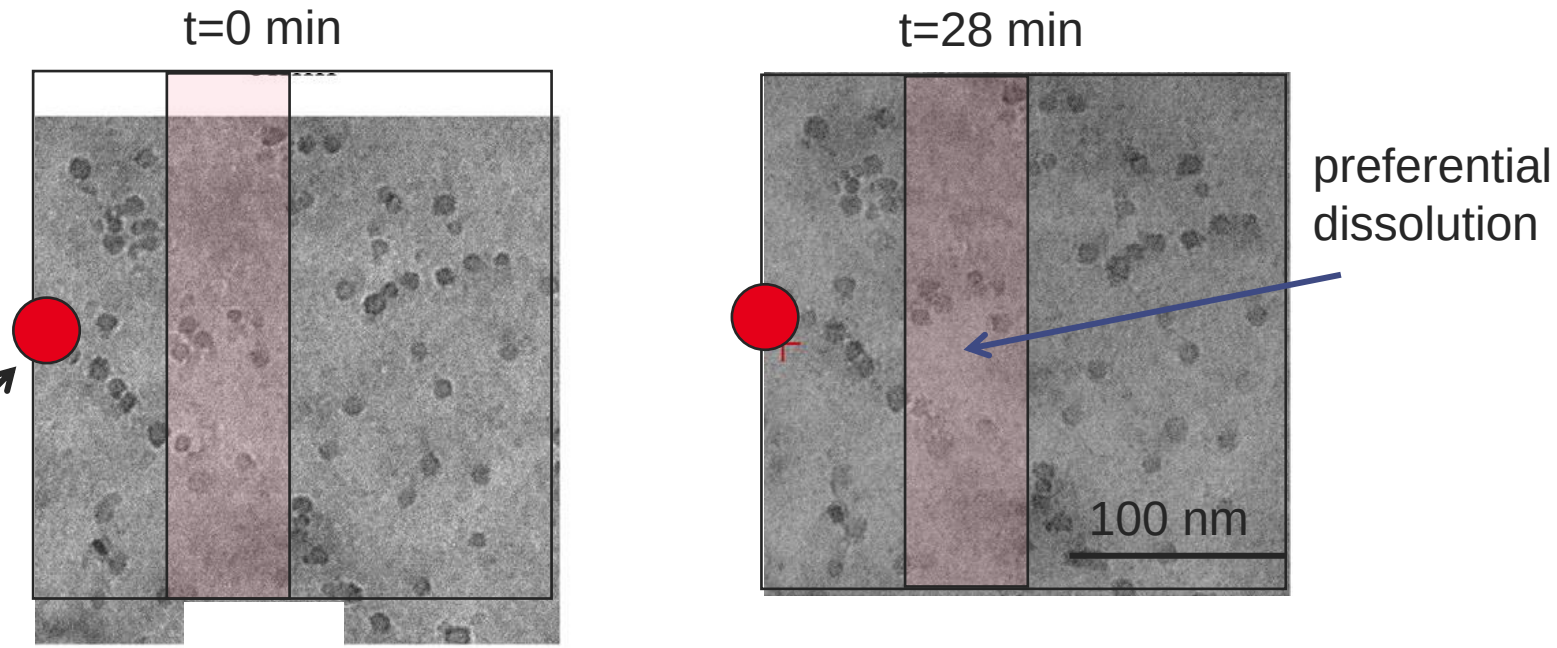

Vacancy-induced dissolution of oxides

T. Schuler et al. PRB 95 (2017) 014113

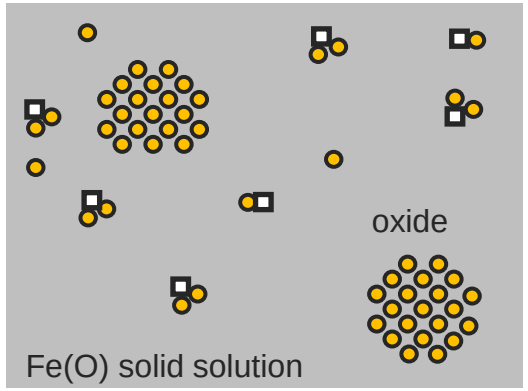

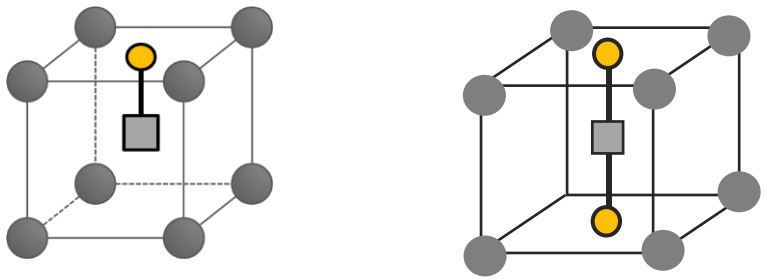

$E_b(VO)$=1.4-1.7 eV $E_b(VO_2)$=3 eV

C. Barouh et al. PRB 90 (2014) 054112

Highly attractive defect-solute clusters stabilise O in the solid solution Fe(O)

Defect-induced dissolution of Fe-based oxide particles

*T. Schuler et al. PRB 95 (2017) 014113

Rate theory model:

$$[V] = \frac{k^2\Omega}{8\Pi r_c} + \sqrt{\left(\frac{k^2\Omega}{8\Pi r_c}\right)^2 + \frac{\Phi\Omega}{4\Pi r_c D_V^{tot}}}$$

Steady state Vacancy treated as a conservative species

Ballistic mixing: effective Temperature concept
(G. Martin, PRB 30,1984)

$$\begin{cases} [X]_{sol}^{cons}(T) = [X]_{sol}^{eq}(T_{eff}) \\ T_{eff} = T(1 + D_{bal} / D_X^{tot}) \end{cases}$$

Non-equilibrium diffusion (non-eq solute clusters from LTE)

$$\begin{cases} D_X^{tot} = \dfrac{[X_0]D_X + m_X[m]D_m}{[X_0] + m_X[m]} \\ D_{bal} = \Phi n_{rep} d_{rep}^2 \end{cases}$$

cluster m containing m_X solutes

Sink strength: $k^2=10^{15}$ m^{-2}

$\delta = [O]_{sol}^{cons} / [O]_{sol}^{eq}$

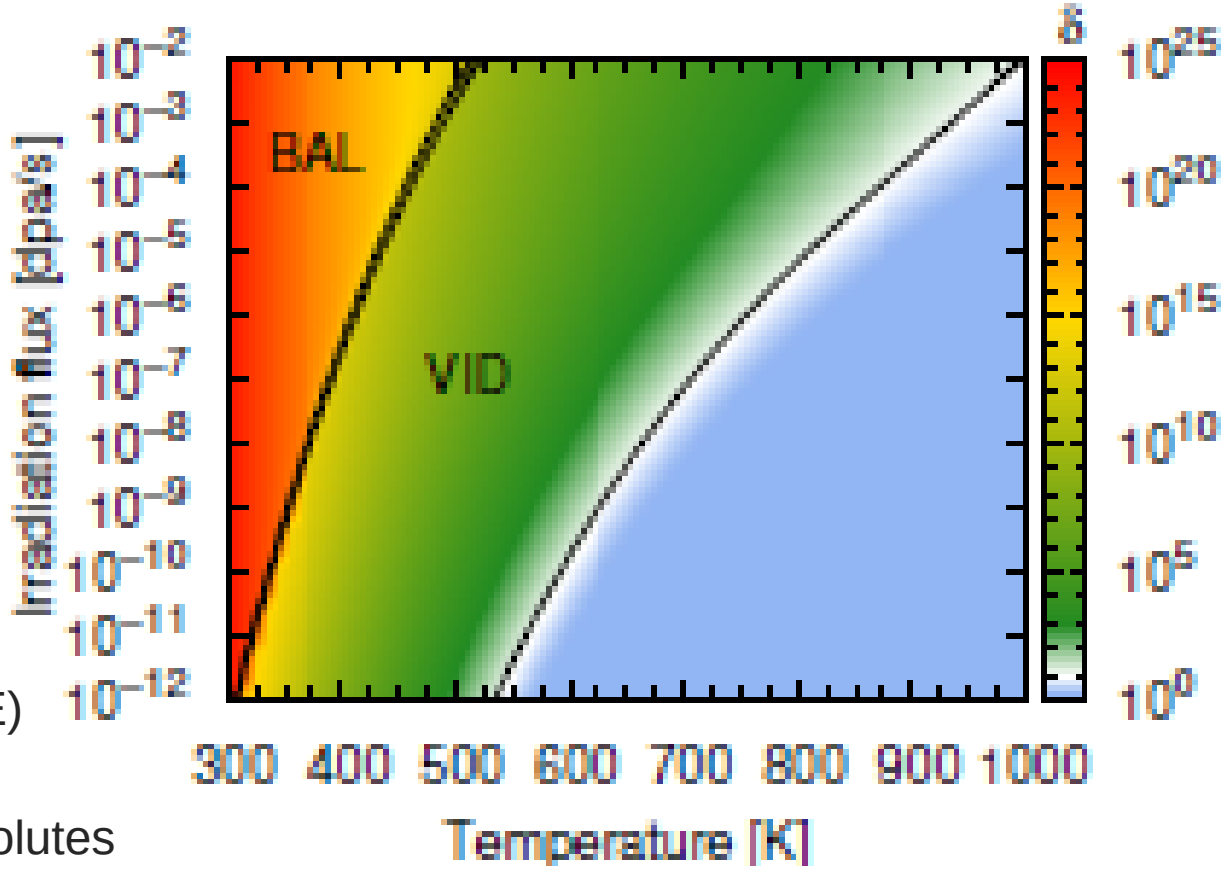

✓ Balistic mixing is dominant at low T and high flux

✓ Vacancy induced dissolution is dominant at medium flux and T

Outline

✓Non-equilibrium Point Defects: diffusion and precipitation driving forces

✓Point-defect induced dissolution of oxide

✓Point-defect induced semi-incoherent precipitation

✓Point-defect formation Gibbs free energy from atomic random sampling

Radiation-induced semi-coherent precipitation

27 MeV Fe^{9+} irradiation,T=400°C

Ultra-pure Fe-3.3Ni

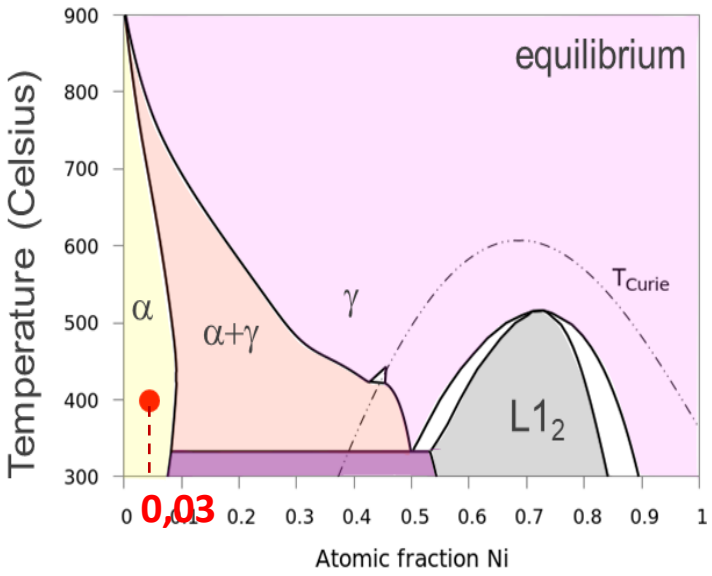

TEM –precipitate population

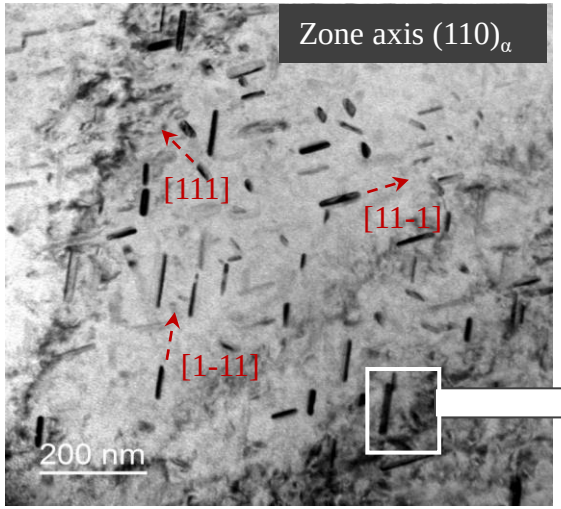

No loop and <111> precipitates in the bcc matrix

HR-TEM image of precipitate

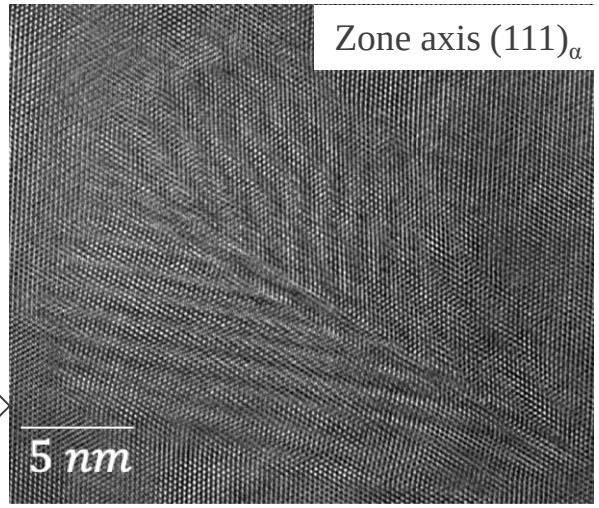

fcc precipitate (austenite)

*L. T. Belkacemi et al., Acta Mat. (2018),

SIA-induced incoherent precipitation mechanism

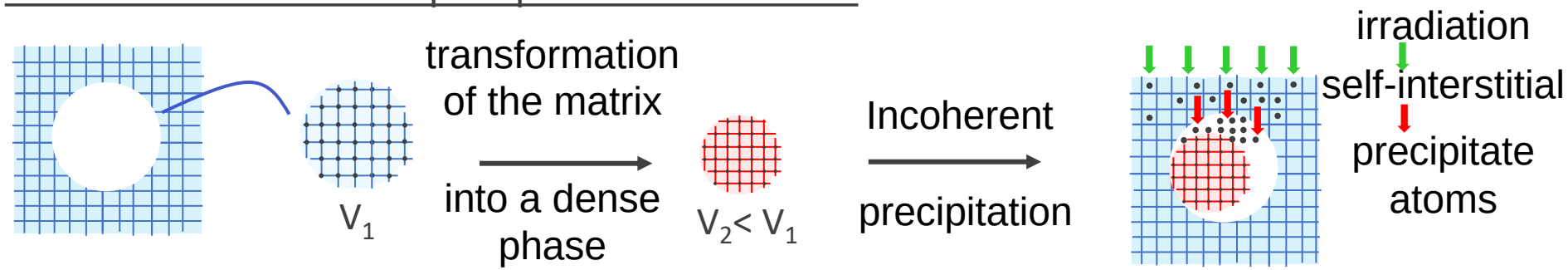

*M. Nastar et al., Commun. Mat, (2021)

SIA transforming into substitutional atoms create lattice sites

Semi-coherent precipitation accommodated by point defects

*Nastar et al., Communication Materials 2 (2021)

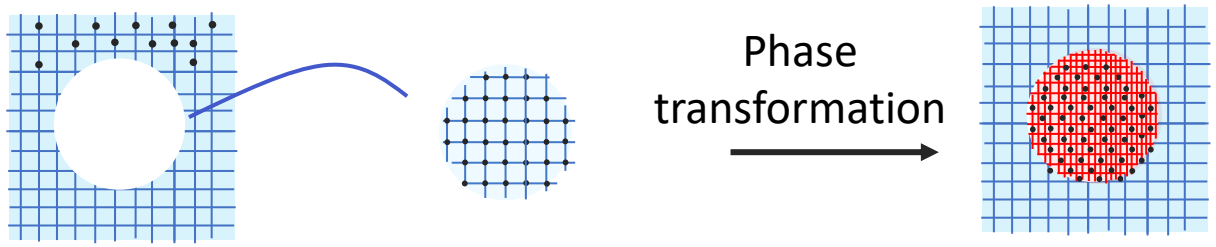

ν_I self-interst. atoms (SIA) + phase α N_α lattice sites → phase γ $(N_\alpha + \nu_I)$ lattice sites

Atomic fraction of SIA accommodating the negative eigenstrain

$$\nu_I = -\varepsilon^* = -(\Omega^\gamma - \Omega^\alpha)/\Omega^\alpha$$

Removal of SIA in excess: an extra precipitation driving force

$$g_\gamma^{RAD} = g_\gamma^{th} + \mu_{SIA}\varepsilon^*$$

$$\Delta g_{prec}^{RAD} = \Delta g_{prec}^{th} + \mu_{SIA}\varepsilon^* < \Delta g_{prec}^{SIA}$$

Defect-induced precipitation driving force
regardless of the sign of the thermal precipitation driving force

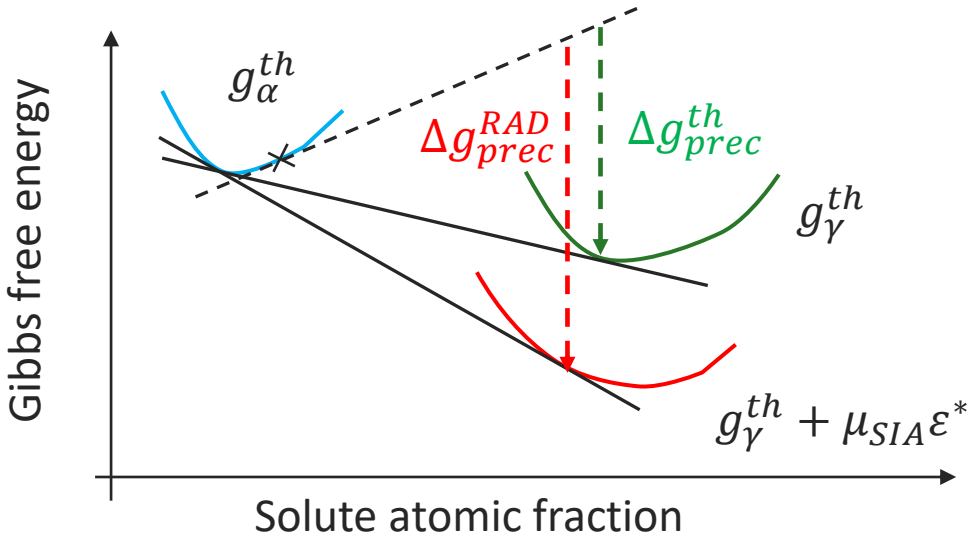

SIA-constrained Gibbs free energy of austenite

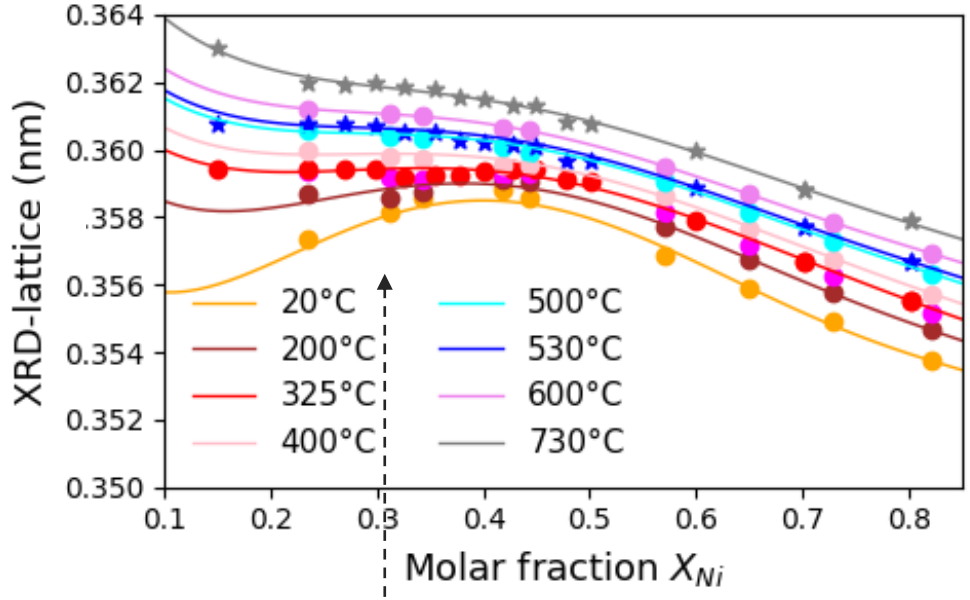

XRD lattice parameters:

*M. Hayase, et al. J. Physical Society of Japan, 34 (1973)

*E. A. Owen at al. Proceeding of the Phys. Soc., 49 (1937)

$T = 400°C$

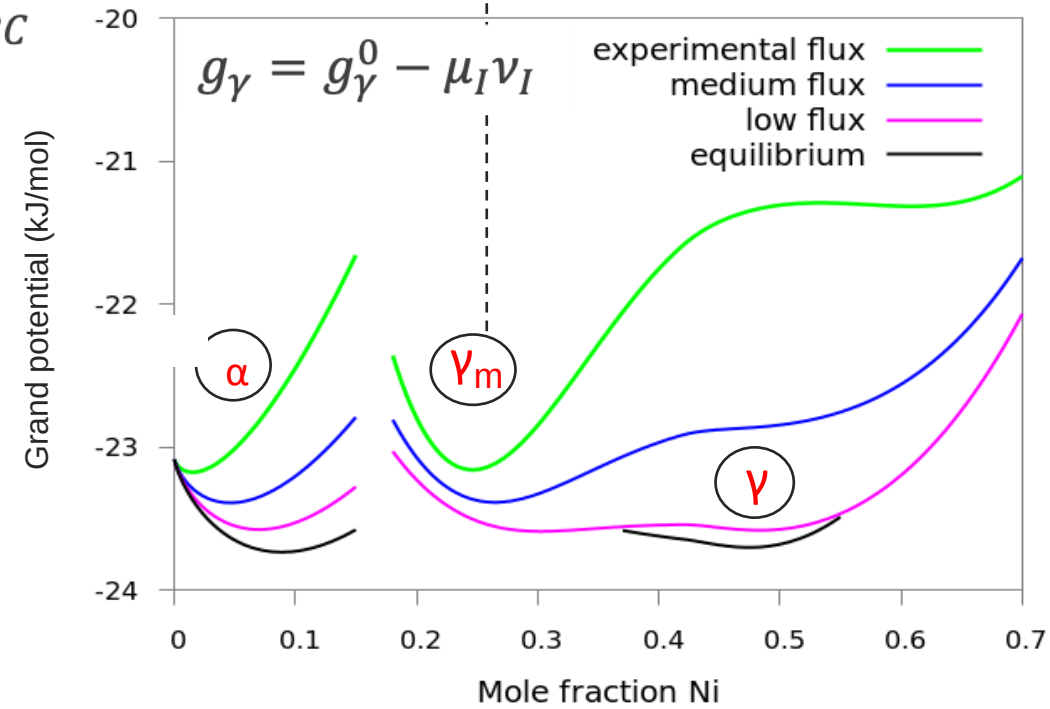

Non-monotonous lattice parameter
With respect to Ni concentration in phase γ

Local minimum of the Gibbs free energy of phase γ at $X_{Ni} = 0.25$

Fodefect-induced metastable FCC solid solution γ_m

SIA-constrained Phase Diagram of Fe-Ni

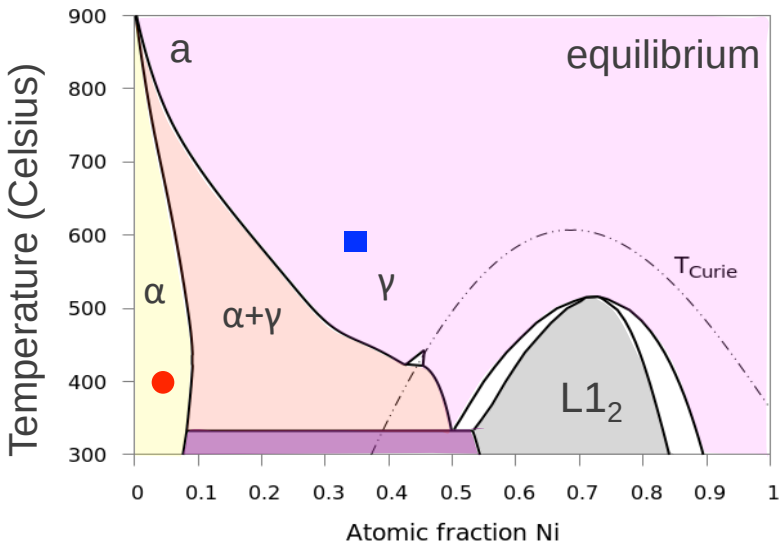

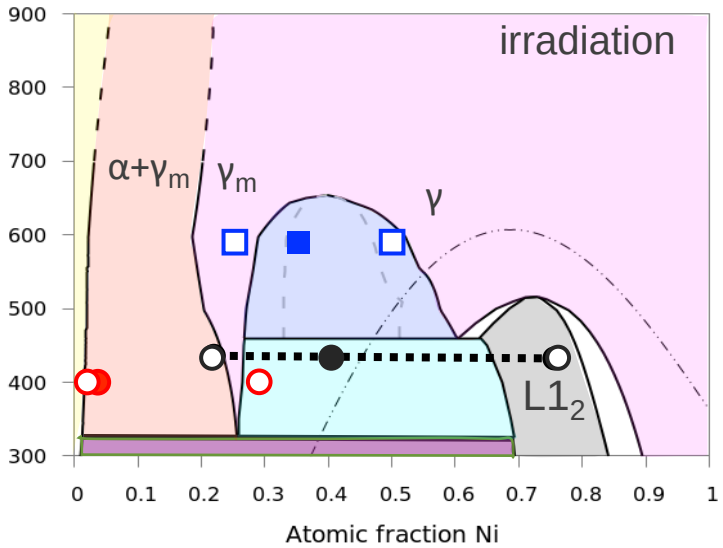

I. Ohnuma et al, CALPHAD, 67, (2019)

Parameters

$k^2 = 10^{13} m^{-2}$

$D_I = 3e^{-0.34/kT} 10^{-6} m^2 s^{-1}$

$C_I = \frac{G}{k^2 D_I}$ $G = 1.25\ 10^{-9} dpa/s$

Experimental observations

- ■ **Garner (1987)* – neutron
- ● **Belkacemi (2018)* – Fe^{9+} ions
- ● **Tencé & Meslin* – Fe^{9+} ions
- this study

- SIA excess induces the precipitation of a metastable phase γ_m
- Model in agreement with experimental observations at T=400 °C in α, and T=600 °C in γ (**Garner et al.*)

**M. Nastar et al., Commun. Mat, (2021)*

Kinetic regimes of Fe-Ni decomposition under irradiation

Fe3Ni_1.2.10^{-5} dpa/s
10dpa_400°C

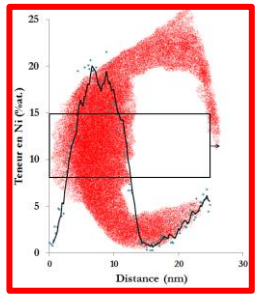

Radiation Induced Seg. of Ni on loops

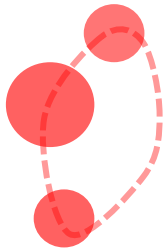

Heterogeneous nucleation of γ on loop

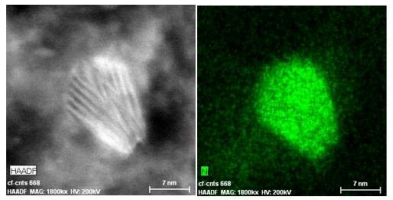

No loops
SIA-induced growth of bulk γ_m

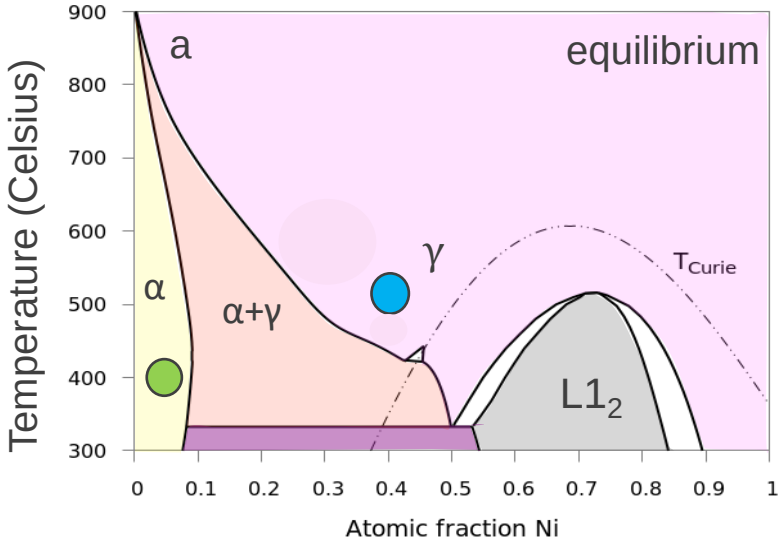

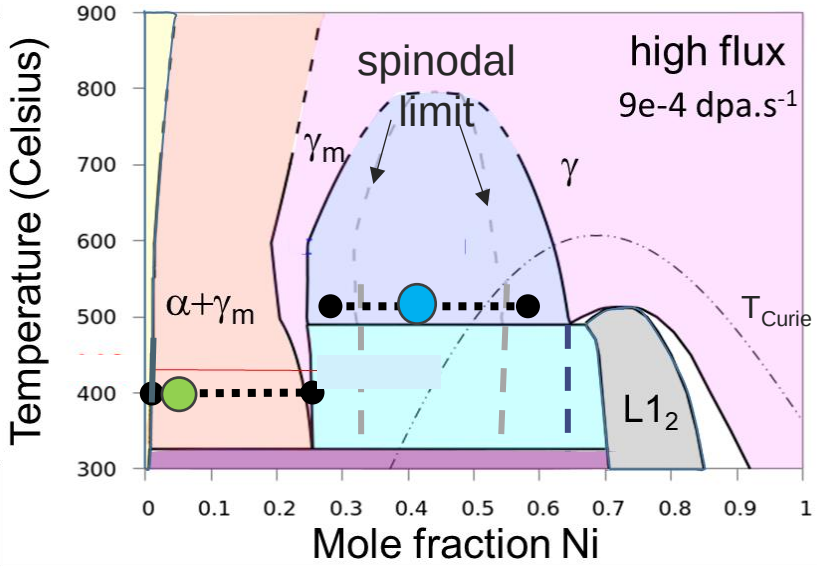

High Voltage in situ TEM
e- irrad. (~5.6 10-^{4}dpa/s)-500°C

Bright field

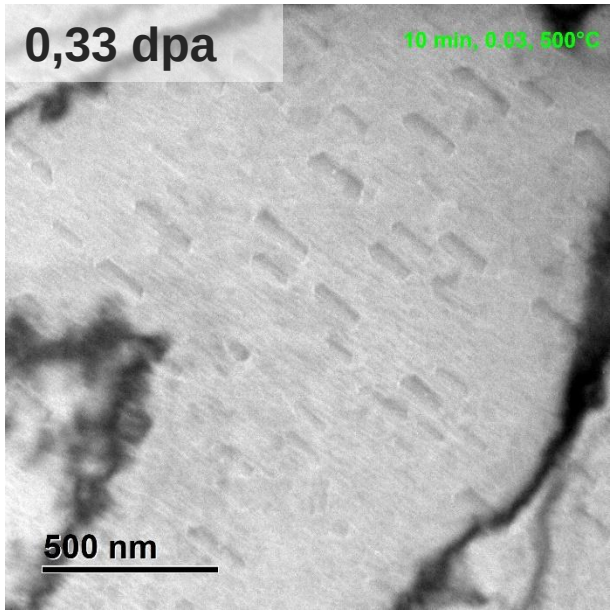

Phase decomposition of FCC phase cannot start on dislocation loops.

Semi-coherent spinodal decomposition: Phase field method ($G_{f,I}$ and $G_{f,V}$: crucial parameters)

Outline

✓Non-equilibrium Point Defects: diffusion and precipitation driving forces

✓Point-defect induced dissolution of oxide

✓Point-defect induced semi-incoherent precipitation

✓Point-defect formation Gibbs free energy from atomic random sampling

Thermodynamics of concentrated FCC Fe-Ni: alloy chemical potential

Widom substitution method on equilibrium configurations

$$\Delta\mu_{AB}^{ex} = -k_B T ln \frac{1}{N_A} \sum_{n\in\Theta_c} \sum_{i\in\Theta_{sites}} P_n \; n_i^A exp\left(-\frac{\Delta E_{n,i}^{A\to B}}{k_B T}\right)$$

$$\Delta\mu_{BA}^{ex} = -k_B T ln \frac{1}{N_B} \sum_{n\in\Theta_c} \sum_{i\in\Theta_{sites}} P_n \; n_i^B exp\left(-\frac{\Delta E_{n,i}^{B\to A}}{k_B T}\right)$$

P_n: equilibrium probability of config. n
$\Delta E_{n,i}^{A\to B}$: Δenergy resulting from the substitution of A by B on site i

Equilibrium sampling: antisymmetry is satisfied

$$\Delta\mu_{AB}^{ex} = -\Delta\mu_{BA}^{ex}$$

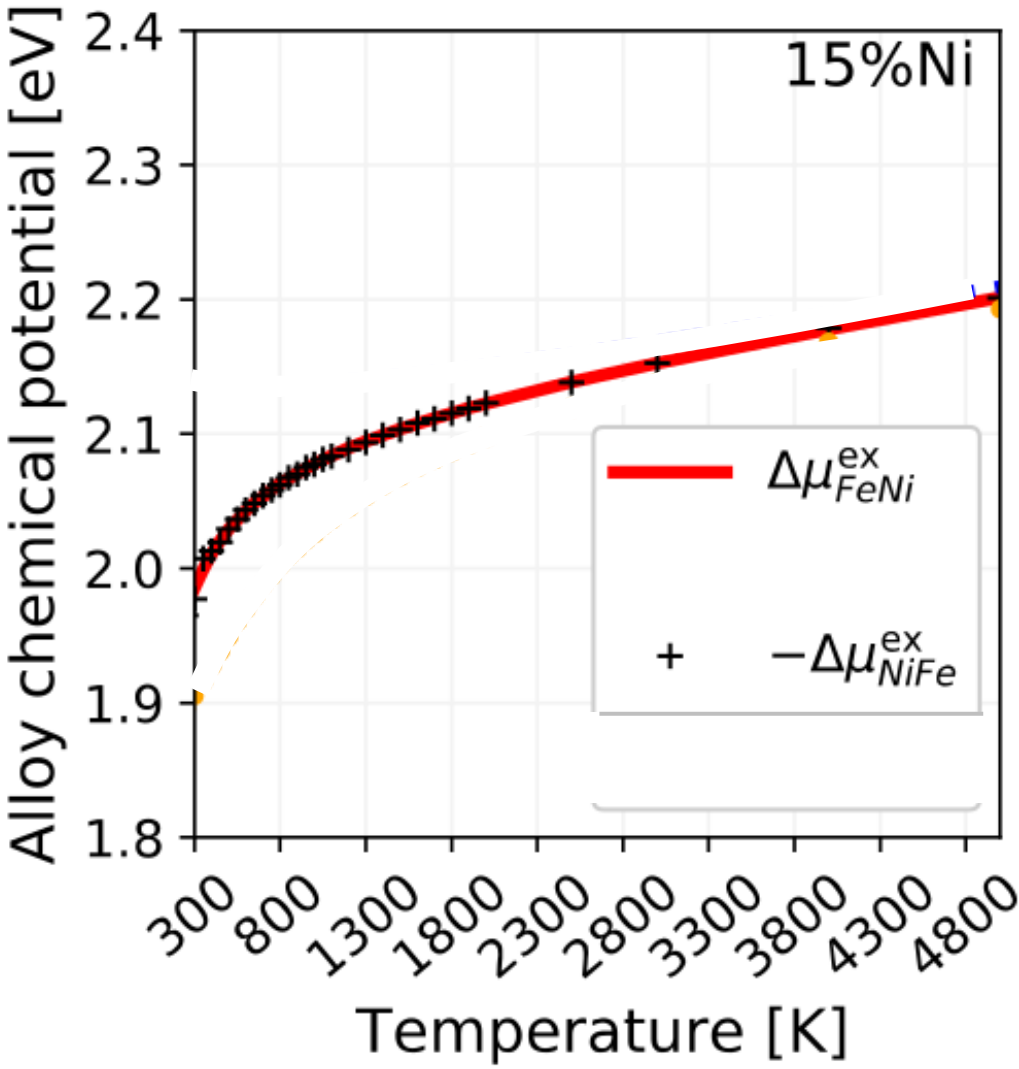

Schuler et al., Acta Materialia 276 (2024) *Li et al., Acta Materialia 281 (2024)*

Thermodynamics of concentrated FCC Fe-Ni: alloy chemical potential

Widom substitution method on random configurations

$$\Delta\tilde{\mu}_{AB}^{ex} = -k_B T ln \frac{1}{N_A} \sum_{n\in\Theta_c} \sum_{i\in\Theta_{sites}} \tilde{P}_n \, n_i^A exp\left(-\frac{\Delta E_{n,i}^{A\to B}}{k_B T}\right)$$

$$\Delta\tilde{\mu}_{BA}^{ex} = -k_B T ln \frac{1}{N_B} \sum_{n\in\Theta_c} \sum_{i\in\Theta_{sites}} \tilde{P}_n n_i^B exp\left(-\frac{\Delta E_{n,i}^{B\to A}}{k_B T}\right)$$

Probabiliy of random atomic configuration n: $\tilde{P}_n = \frac{1}{\Omega_c}$

Antisymmetry is not satisfied: $\Delta\mu_{AB}^{ex} A \neq -\Delta\mu_{BA}^{ex}$

Without SRO (random atomic configurations), alloy chemical potentials are not consistent

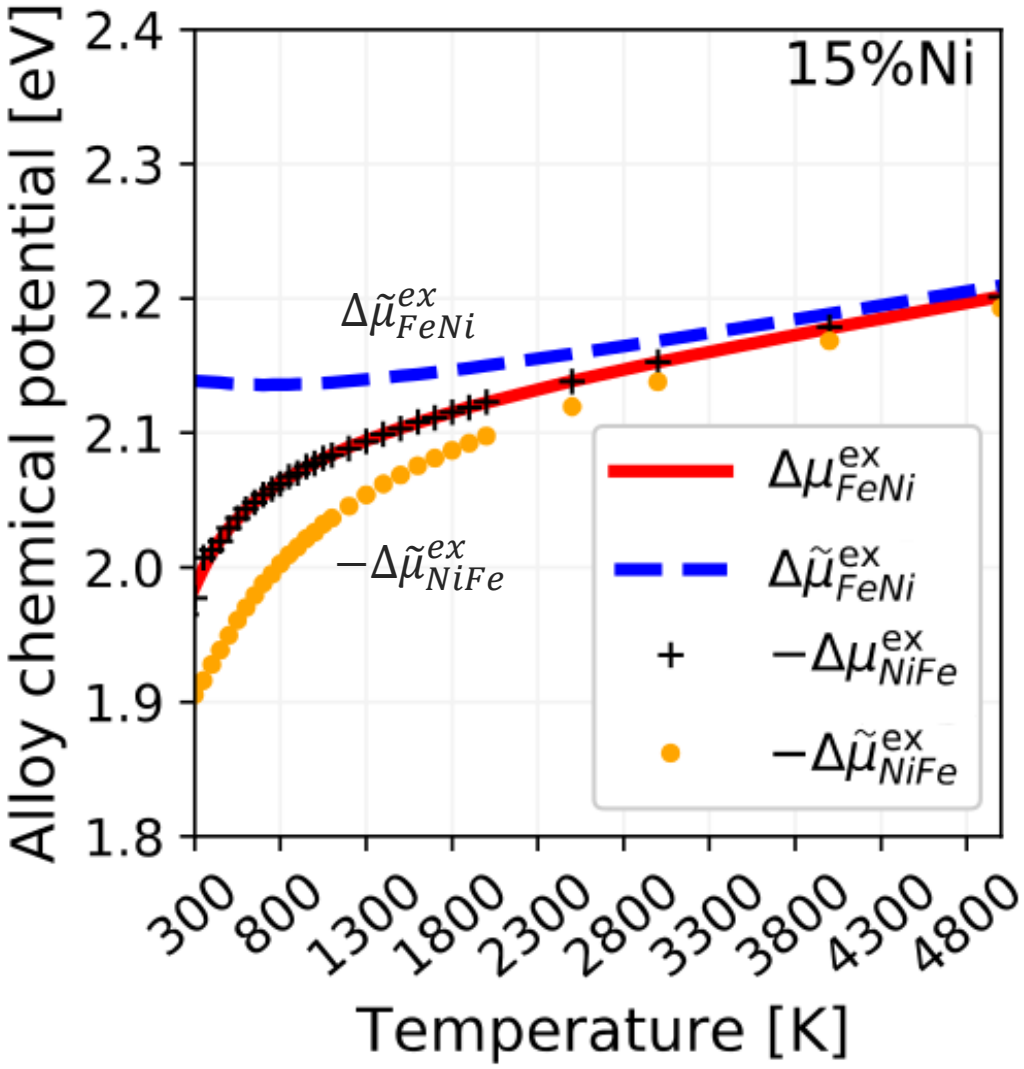

Schuler et al., Acta Materialia 276 (2024) *Li et al., Acta Materialia 281 (2024)*

Thermodynamics of concentrated FCC Fe-Ni

Schuler et al., Acta Materialia 276 (2024)

Random-sampling alloy chemical potentials

$\Delta^c \tilde{\mu}_{AB}^{ex}$ and $-\Delta^c \tilde{\mu}_{AB}^{ex}$ in function of the equil. $\Delta\mu_{BA}^{ex}$

Modifed random-sampling alloy chemical potential

$$\Delta^c \tilde{\mu}_{AB}^{ex} = \frac{x_A \Delta\tilde{\mu}_{AB}^{ex} - x_B \Delta\tilde{\mu}_{BA}^{ex}}{x_A + x_B}$$

- ✓ Antisymmetry is satisfied
- ✓ Good quantitative agreement between and $\Delta^c \tilde{\mu}_{AB}^{ex}$ and $\Delta\mu_{BA}^{ex}$

300 K< T < 5000 K and $0 < C_{Ni} < 1$

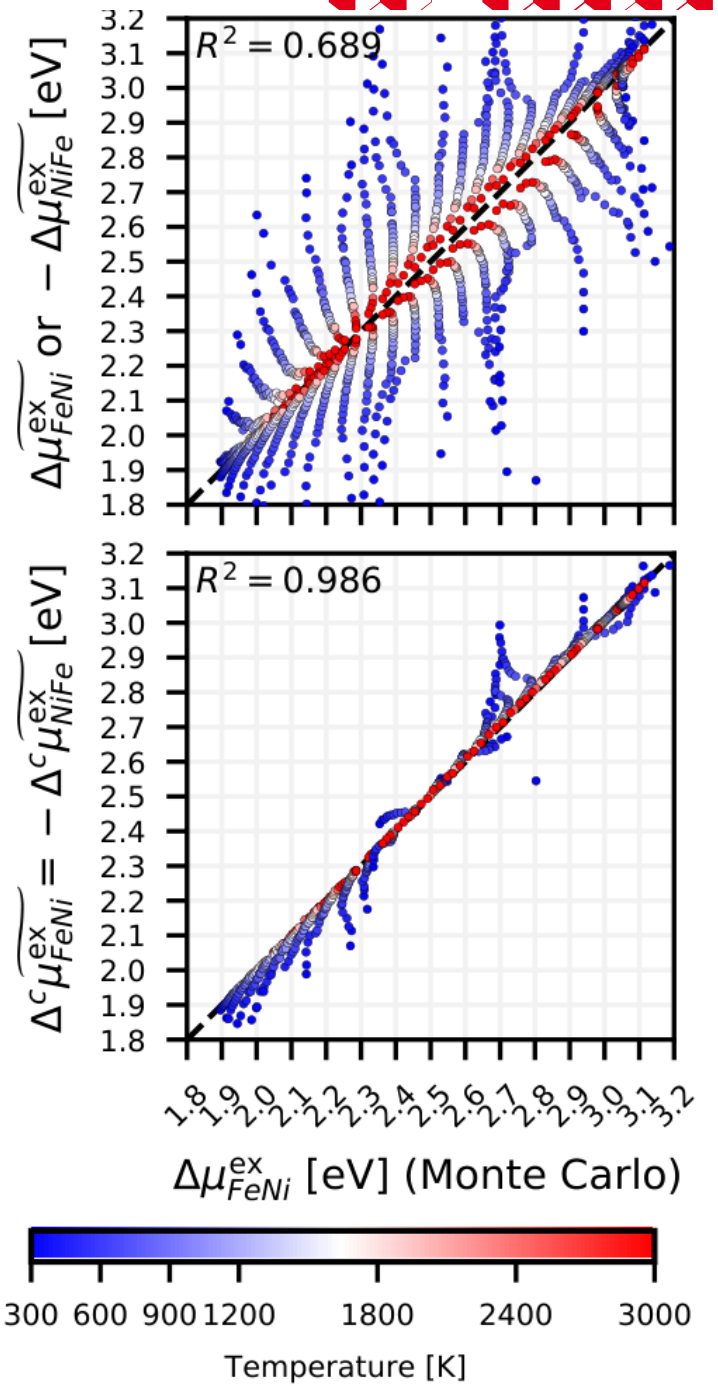

Thermodynamics: Substitution Energy -DOS

<u>Energy Spectra of SE-DOS:</u>

random-SEDOS ≡ equilibrium SE-DOS

<u>Corrected random SE-DOS:</u>

Asumption: SE-DOS are normal distributions

Corrected random SE-DOS in good agreement with eq. SE-DOS

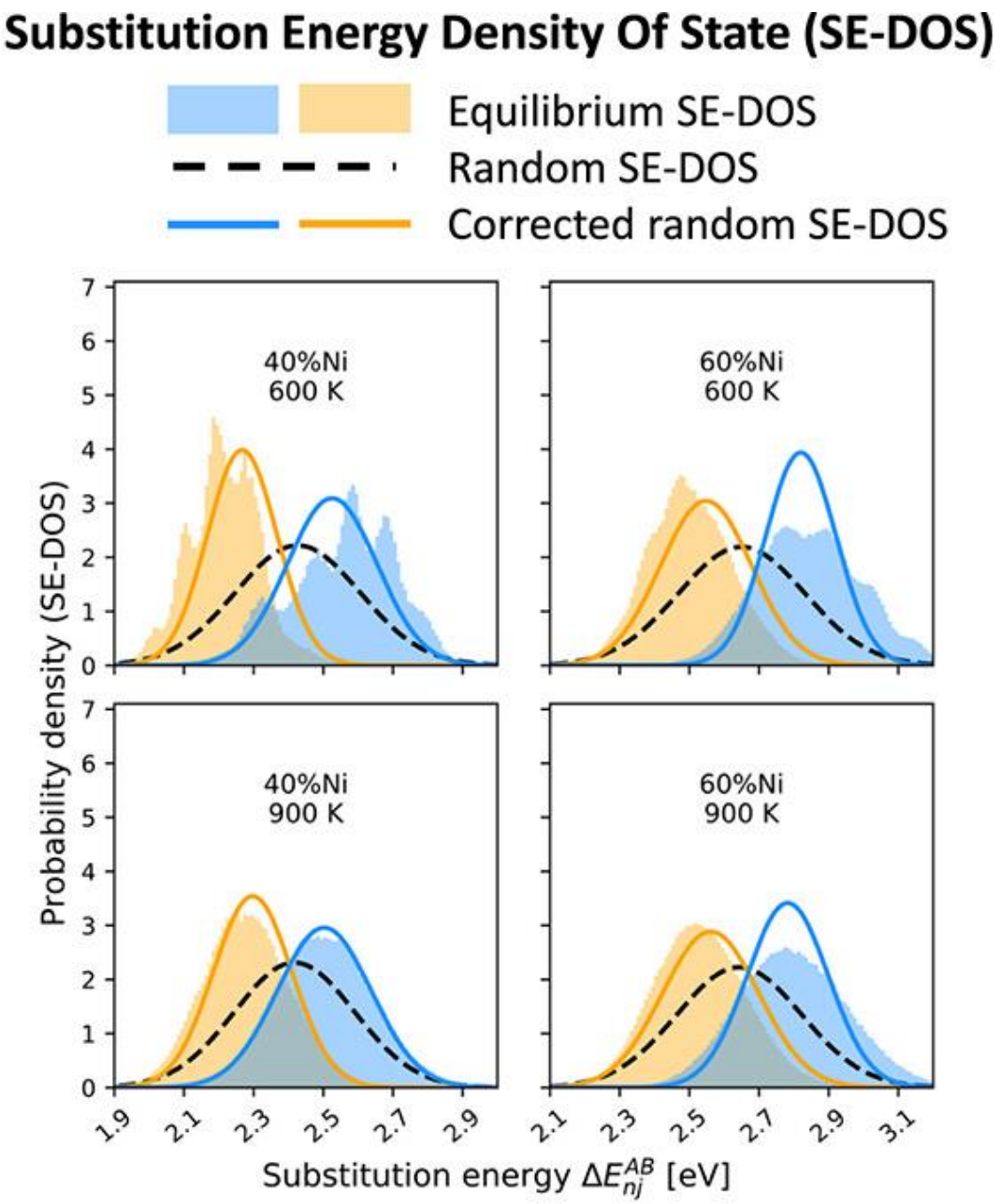

Schuler et al., Acta Materialia 276 (2024)

Thermodynamics of concentrated alloys: vacancy equilibrium concentration

$$G_f\,(A) = \Delta\mu_{AV}^{ex} + \mu_A^{ex} = -k_B T\ \ln \frac{1}{N_A} \sum_{n\in\Theta_c} \sum_{i\in\Theta_{sites}} \tilde{P}_n\, n_i^A exp\left(-\frac{\Delta E_{n,i}^{A\to V} + \mu_A^{ex}}{k_B T}\right)$$

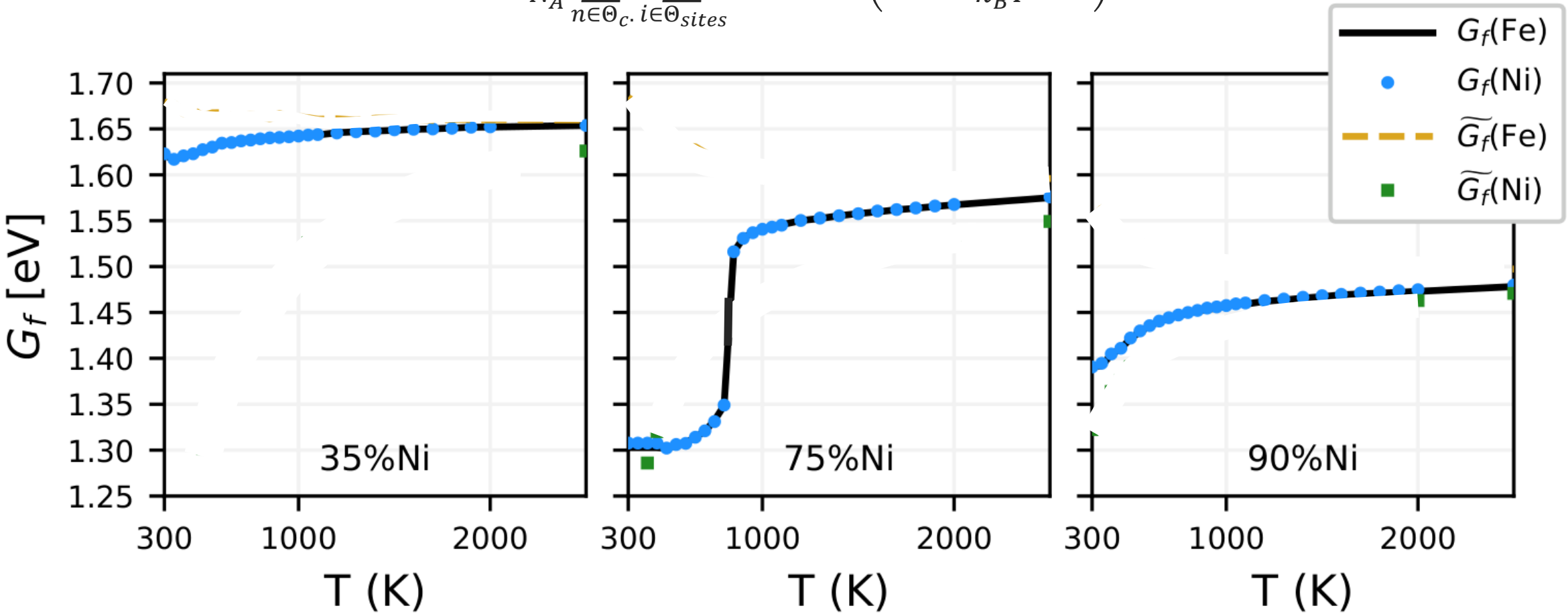

Without SRO, G_f(Fe) and G_f(Ni) are not inconsistent

Schuler et al., Acta Materialia 276 (2024) *Li et al., Acta Materialia 281 (2024)*

Thermodynamics of concentrated alloys: vacancy equilibrium concentration

$$\widetilde{G_f}(A) = \Delta\mu_{AV}^{ex} + \mu_A^{ex} = -k_B T \ \ln \frac{1}{N_A} \sum_{n \in \Theta_c} \sum_{i \in \Theta_{sites}} \tilde{P}_n \, n_i^A exp\left(-\frac{\Delta E_{n,i}^{A \to V} + \mu_A^{ex}}{k_B T}\right)$$

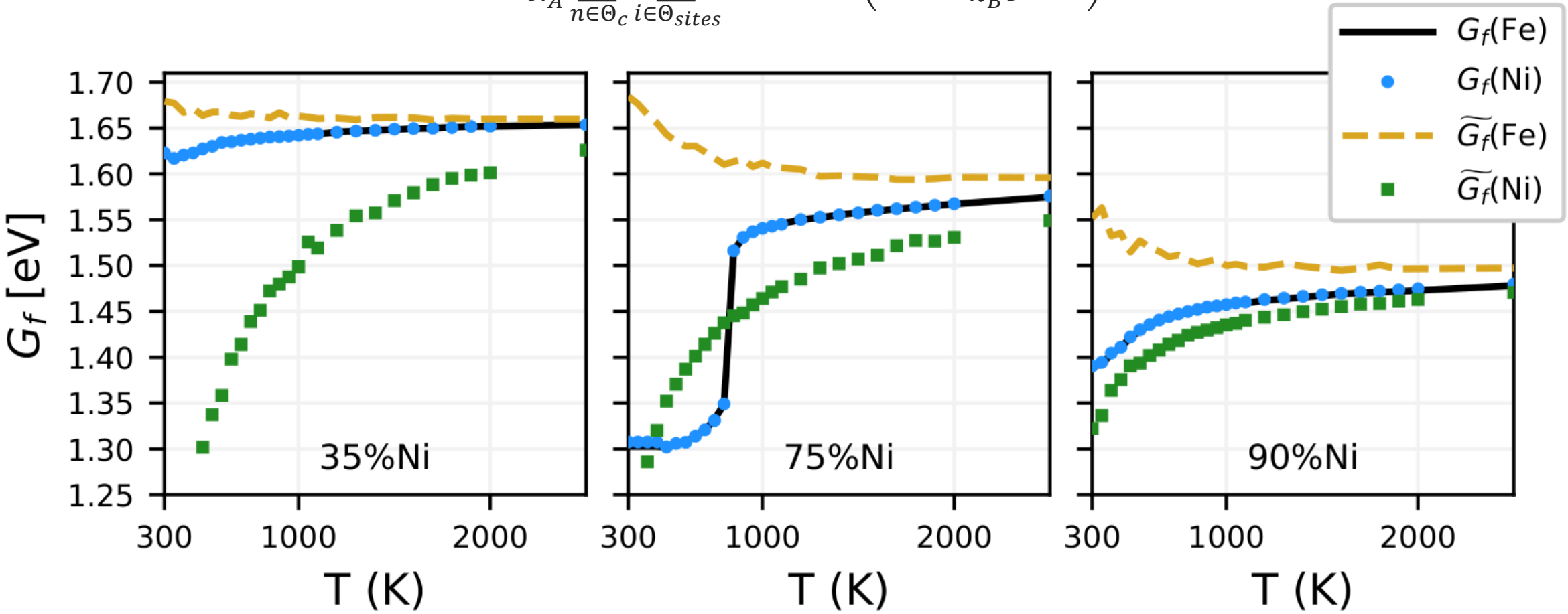

Without SRO, $G_f(\mathrm{Fe})$ and $G_f(\mathrm{Ni})$ are not inconsistent

Schuler et al., Acta Materialia 276 (2024) *Li et al., Acta Materialia 281 (2024)*

Thermodynamics of concentrated alloys: vacancy equil. concentration

Modified alloy chemical potential: $\Delta^c \tilde{\mu}_{AB}^{ex}$

Modified vacancy Gibbs free energy: $\widetilde{G_f}$-mean and $\widetilde{G_f^c}$

$\widetilde{G_f}$ mean only: infinite-Temprature approximation
$\widetilde{G_f^c}$ - VF-DOS are normal distributions

- ✓ Antisymmetry is satisfied
- ✓ Satisfying agreement between $\widetilde{G_f^c}$ and equilibium G_f
- ✓ Discrepancy stems from the hyp. of normal VF-DOS

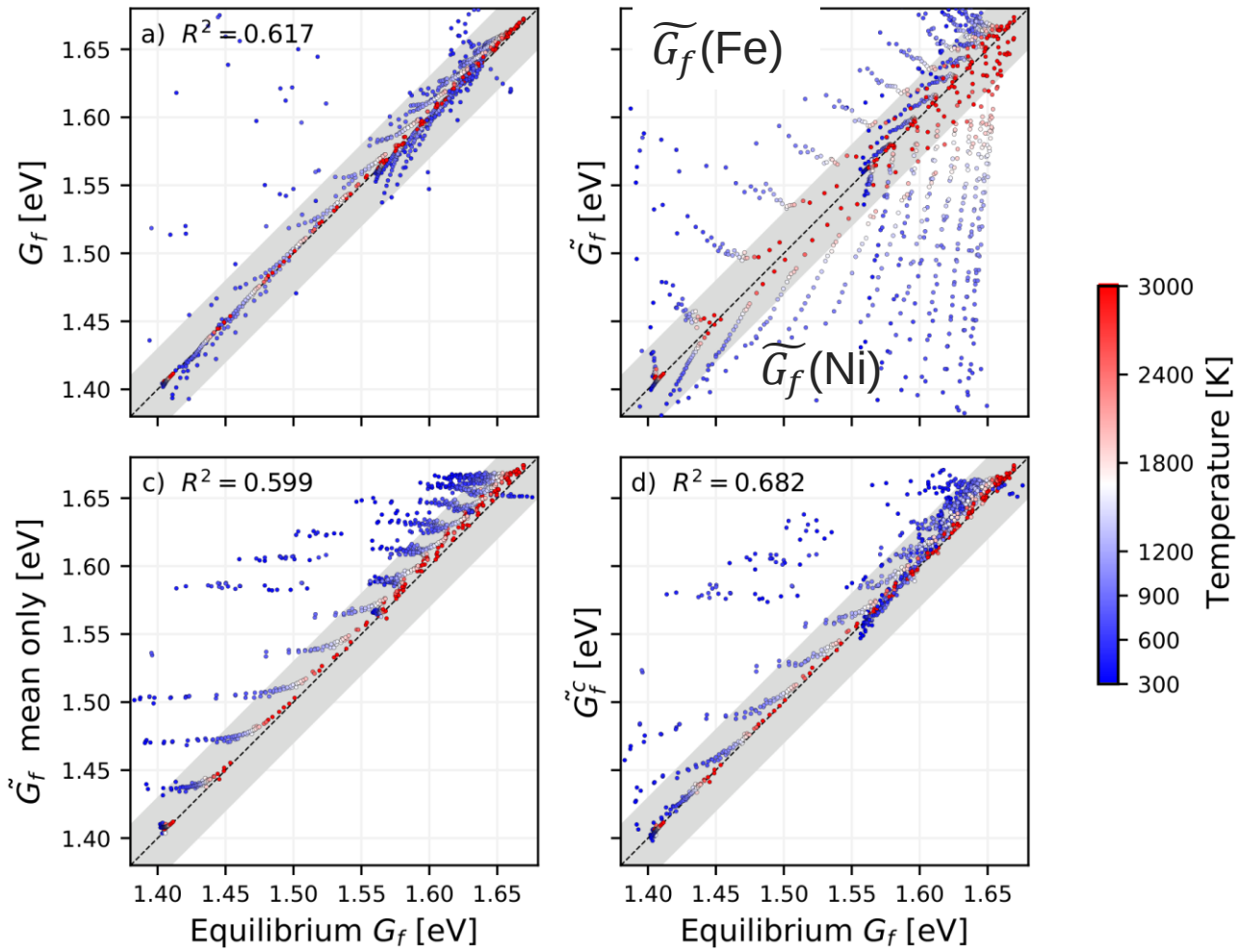

Schuler et al., Acta Materialia 276 (2024) *Li et al., Acta Materialia 281 (2024)*

Conclusion and perspectives
Dynamical coupling between RIS/precipitation and microstructure evolution

Conservative point defect: thermodynamic driving force of semi-coherent precipitation under irradiation

✓ An excess of defect in attraction with solute atoms may increase the solute solubility limit (FeO)

Non conservative point defect: thermodynamic driving force of semi-coherent precipitation under irradiation

✓ An excess of SIA / Vacancy induces the precipitation of phases denser / less dense than the matrix

✓ Semi-coherent precipitates are strong point defect sinks leading to absorption biases and specific μstructure

Radiation-induced segregation: often a catalytic mechanism of RIP

Prospects

✓ Thermodynamics and diffusion of PDs in concentrated alloys (SRO magnetism, vibrational entropy, etc.)

✓ Non expected phases transformations to be revisited from the perspective of point defect-induced precipitation: Unexpected phases in W-Re : χ phase instead of the less rich Re σ phase, incubation dose of blooming , phases (phase G and C15), Change of precipitate compo and re-precipitation in Zr-Nb, HEA, etc.

✓ Mechanisms of nucleation of radiation-induced semi-coherent precipitate: role of RIS, spinodal decomposition

T. Schuler et al. JAP vol. 132 (2022) 080903

Thank you

Acknowledgments: T. Schuler, E. Meslin, F. Soisson, T. Jourdan, C. C. Fu, M. Loyer-Prost, B. Décamps

PhD students: L. Huang, L. Belkacemi, Q. Tencé, A. Dartois

EUROFUSION Consortieum, H2020 EURATOM GEMMA, INNUMAT

CEA SACLAY

91191 Gif-sur-Yvette Cedex

France

maylise.nastar@cea.fr

Standard. + 33 1 69 08 60 00